Fluorocholesterols, in contrast to hydroxycholesterols, exhibit interfacial properties similar to cholesterol

John M. Kauffman,* Philip W. Westerman,† and Martin C. Carey[1,*]

Department of Medicine,* Harvard Medical School, Harvard Digestive Diseases Center, and Division of Gastroenterology,* Brigham and Women's Hospital, Boston, MA 02115; and Department of Biochemistry and Molecular Pathology,† Northeastern Ohio Universities' College of Medicine, Rootstown, OH 44272

Abstract **We used an automated Langmuir-Pockels surface balance to characterize the air–water interfacial properties of cholesterol (CH) and its derivatives with hydrophilic OH and F substitutions at isologous sites on the sterol body or side chain. We studied 6-fluorocholesterol, 25-fluorocholesterol, 25,26,26,26,27,27,27-heptafluorocholesterol, 7α-hydroxycholesterol, 7β-hydroxycholesterol, 25-hydroxycholesterol and 27-hydroxycholesterol, alone and in mixtures with 1-palmitoyl-2-oleoyl-*sn*-3-glycero-phosphocholine (POPC). Pressure–area isotherms of the fluorocholesterols were essentially indistinguishable from CH and all condensed POPC monomolecular layers (monolayers) to variable degrees. Both nucleus-substituted hydroxycholesterols formed expanded monolayers, with lift-offs from baseline 22–26 Å²/molecule larger than CH, suggesting interfacial tilting; furthermore, in binary mixtures, they condensed POPC monolayers less than CH. In contrast, the side chain hydroxylated CHs were oriented horizontally in the interface at large molecular areas, and became vertical below 140 Å²/molecule with the side chain-OH rather than 3-OH group anchored in the subphase, as evidenced by low collapse pressures and smaller molecular areas than CH. Both side chain hydroxycholesterols expanded POPC monolayers at molar ratios <30%, but induced condensation with higher ratios, suggesting that OH-acyl chain (POPC) repulsion is superceded at higher mole fractions by lateral phase separation and intersteroidal H-bonding. These studies predict that fluorocholesterols should exhibit intramembrane spatial occupancy nearly identical to CH, whereas nucleus and especially side chain hydroxycholesterols will perturb membrane lipid packing notably.**—Kauffman, J. M., P. W. Westerman, and M. C. Carey. **Fluorocholesterols, in contrast to hydroxycholesterols, exhibit interfacial properties similar to cholesterol.** ***J. Lipid Res.*** **2000.** 41: **991–1003.**

Supplementary key words phosphatidylcholine • surface potential • condensation • isotherm • orientation • surface balance • spectroscopic imaging

Single atomic substitutions of fluorine (F) for hydrogen (H) in organic compounds result in a highly stable covalent F-carbon bond with little steric change (1). The effective van der Waal's radii of H and F in bonding with carbon (C) are 1.2 and 1.4 Å (2), respectively. However, in contrast to the other halogens, F is considerably more electronegative (3), potentially conferring a hydrophilic character to hydrocarbon ring systems or acyl chains. Depending on the proximity of the F substituent to functional groups, fluorinated analogues of biological molecules may be recognized by transport proteins, enzymes, and receptors, and therefore may follow metabolic and physical–chemical pathways like the native compound. Because of its electron-withdrawing effects, F substitution near a functional group can also perturb metabolism of the fluoro-compound. This can result in compounds with potentiated biological activity, examples being fluorinated anticancer and anti-viral agents, and steroids with increased anti-inflammatory and glycogenic properties (4, 5). Several monofluorinated CHs (FCH) have been synthesized previously, with fluorination on either the side chain or nucleus (6–9). The vicinal effect of F substitution on enzymatic processes is demonstrated by 6-fluorocholesterol (6FCH), whereby substitution of F for H at the C-6 position of CH results in little effect on acyl-CoA:cholesterol acyltransferase (ACAT) activity at the C-3 position, whereas CH 7α-hydroxylase is inhibited (10).

Studying monolayers of insoluble amphiphilic molecules (11), such as phosphatidylcholines (PC) and CH, permits characterization of size, interactions, and orientation of the molecules, with the configurations being analogous to those in a model hemimembrane. Analysis of surface pressure–area ($\pi - A$) isotherms has characterized the interfacial properties of many lipids (12), including those of biological relevance such as CH, several hydroxycholesterols (OHCHs) (13), unconjugated bile acids (14),

Abbreviations: F, fluorine; CH, cholesterol; FCH, fluorocholesterol; OHCH, hydroxycholesterol; 6FCH, 6-fluorocholesterol; 25FCH, 25-fluorocholesterol; HeptaFCH, 25,26,26,26,27,27,27-heptafluorocholesterol; 7αOHCH, 7α-hydroxycholesterol; 7βOHCH, 7β-hydroxycholesterol; 25OHCH, 25-hydroxycholesterol; 27OHCH, 27-hydroxycholesterol; POPC, 1-palmitoyl-2-oleoyl-*sn*-glycero-3-phosphocholine; PC, phosphatidylcholine; π, surface pressure; and *A*, area.

[1] To whom correspondence should be addressed.

sphingomyelins (15), galactocerebrosides (16), several PCs, and various binary and ternary mixtures of these lipids (17–21). A well-documented effect of CH on monolayers of phospholipids, particularly PC unsaturated at the *sn*-2 position (22), is condensation, whereby the mean molecular area of the mixed system is less than the average of the individual components in a simple monolayer.

F-substituted compounds including serotonin (23) and bile acids (24) have been proposed as tracer molecules for electron spectroscopic imaging, a technique whereby mapping of single atoms in biological structures is approaching realization (25). We have synthesized FCHs to determine how closely they mimic CH alone and in their interactions with 1-palmitoyl-2-oleoyl-*sn*-3-glycero-phosphocholine (POPC), a common membrane phospholipid. Here we report our monolayer investigations of fluorinated analogues of CH: 6-fluorocholesterol (6FCH), 25-fluorocholesterol (25FCH), and 25,26,26,26,27,27,27-heptafluorocholesterol (heptaFCH). Surface pressures (π), dipole moments (mD) and viscosities, all measured as functions of surface area (A), suggest that these fluorinated molecules closely mimic the molecular and hemimembrane behavior of CH, both alone and in mixtures with POPC. In contrast, a stronger electronegative substitution, OH, at similar sites on the sterol nucleus and side chain induces tilting of the former and inversion of the latter, with side chain more than nucleus-hydroxylated CHs perturbing interactions with POPC.

EXPERIMENTAL PROCEDURES

Materials

The monofluorinated sterols, 6FCH and 25FCH, were synthesized by fluorination of the 6-keto group of 6-ketocholestanol-3-acetate and the 25-hydroxy group of 25-hydroxycholesteryl-3-acetate by diethylaminosulfur trifluoride (10, 26). High-resolution ^{19}F, ^{13}C, and ^{1}H NMR spectroscopy confirmed molecular identity. Final purification of both FCHs was performed by reverse-phase HPLC using an Altex Ultrasphere ODS 25 cm × 10 mm, 5 μm column and a methanol–isopropanol 70:30 solvent system. HeptaFCH (27) was generously provided by Dr. William Wilson (Rice University, Houston, TX). The 7α-, 7β-, 25- and 27-hydroxycholesterols (7αOHCH, 7βOHCH, 25OHCH, and 27OHCH) were purchased from Steraloids (Wilton, NH). Synthetic POPC was purchased from Avanti Lipids (Alabaster, AL). CH was obtained from Nu-Chek Prep (Austin, MN) and purified by preparative HPLC using a chloroform–acetonitrile–methanol 1:1:1 (vol:vol:vol) solvent system. All lipids were >99% pure by reversed phase thin layer chromatography on octadecylsilane plates from Whatman (Maidstone, England) using isopropanol–acetonitrile 1:1 (vol:vol). Organic solvents, purchased from Sigma Chemicals Co. (St Louis, MO), were HPLC grade and free of surface active impurities, as assessed by layering 100 μl solvent onto the subphase and measuring surface pressures during film compression. Water was distilled after reverse osmosis and filtered through activated charcoal. Sodium chloride was roasted at 600°C for 6–8 h to remove organic impurities. All glassware was alkali-acid washed in EtOH–2 m KOH 1:1 (vol:vol) and in 1 m HNO_3 overnight, followed by prolonged rinsing with distilled water.

Solutions

To prepare spreading solutions, stock solutions were composed in chloroform at an estimated solute concentration of 12–14 mg/ml. Solutions were then filtered through an organic solvent-resistant Millex-LCR_{13} 0.5 μm filter (Millipore, Bedford, MA). Dry weights were measured using quadruplicate 100 μl volumes with evaporation of the solvent under reduced pressure in a vacuum desiccator at 35°C for 1 h. After venting the desiccator, lipid weights were measured to 5 decimal places at frequent intervals on an analytical balance for a total of 3 min, followed by extrapolations to zero time. Spreading solutions were prepared with benzene to final concentrations of 0.2 and 0.3 mm. To prevent oxidation, all spreading solutions were stored under N_2 at 4°C for a period no longer than 6 weeks.

Molecular areas and surface potential measurements

π–A isotherms were obtained using an 8.5 × 36.5 cm Teflon-lined Langmuir-Pockels surface balance with computer-controlled barriers (KSV, Finland) as previously described (21). We made the following minor modifications to the procedure. Monomolecular layers of CH, FCHs, or OHCHs, alone and in binary mixtures with POPC, were spread using 100 μl Hamilton glass syringes (Reno, NV) on a subphase of 5 m NaCl at pH 3 (not pH 2 as in ref. 21), T = 21 ± 0.5°C. All solvents were allowed to evaporate for 3 min prior to compression of the monolayer. Lift-offs and collapse points were defined as the intersection of tangents on each side of the curves encompassing areas where isotherms deviate in a first-order fashion. Between 3 and 5 isotherms were run for each lipid individually and in binary mixtures, with lift-off areas reproducible to within 1%. At the conclusion of the runs, roasted talc ($Mg(SiO_4)_3$) was sprinkled onto the compressed monolayer, and its movement under a fine air jet was used to assess surface viscosity. Failure of the talc to move suggests a monolayer that is in the gel or crystalline state, whereas free movement suggests the liquid state (19). Surface potentials were obtained with an α-emitting polonium source as described previously (21), and normalized by the surface potential per molecule. The surface dipole moment (mD) was calculated according to the formula of Gaines (12).

Software for molecular modeling

ChemDraw Pro and Chem3D Std (Cambridge Scientific, Cambridge, MA) were used to develop two- and three-dimensional models of CH, FCHs, and OHCHs. Energy minimization of three-dimensional models was performed where appropriate.

RESULTS

Nucleus-substituted cholesterols

Figure 1 depicts π–A isotherms (A) and surface dipole moments (B) for monolayers of pure CH, 6FCH, 7αOHCH, and 7βOHCH. The isotherms (Fig. 1A) of both 6FCH and CH are essentially identical during compression with slight expansion of 6FCH noted in all runs (n = 5). Lift-offs occur at 39.5 and 40 $Å^2$/molecule for CH and 6FCH respectively, and both surface pressures rise steeply into a solid, condensed film, consistent with vertical orientation of the molecules at the interface. Isotherms of 7αOHCH and 7βOHCH demonstrate distinctly different patterns from each other and from 6FCH and CH. They display lift-offs at much larger molecular areas (7βOHCH > 7αOHCH), with complex behavior during compression,

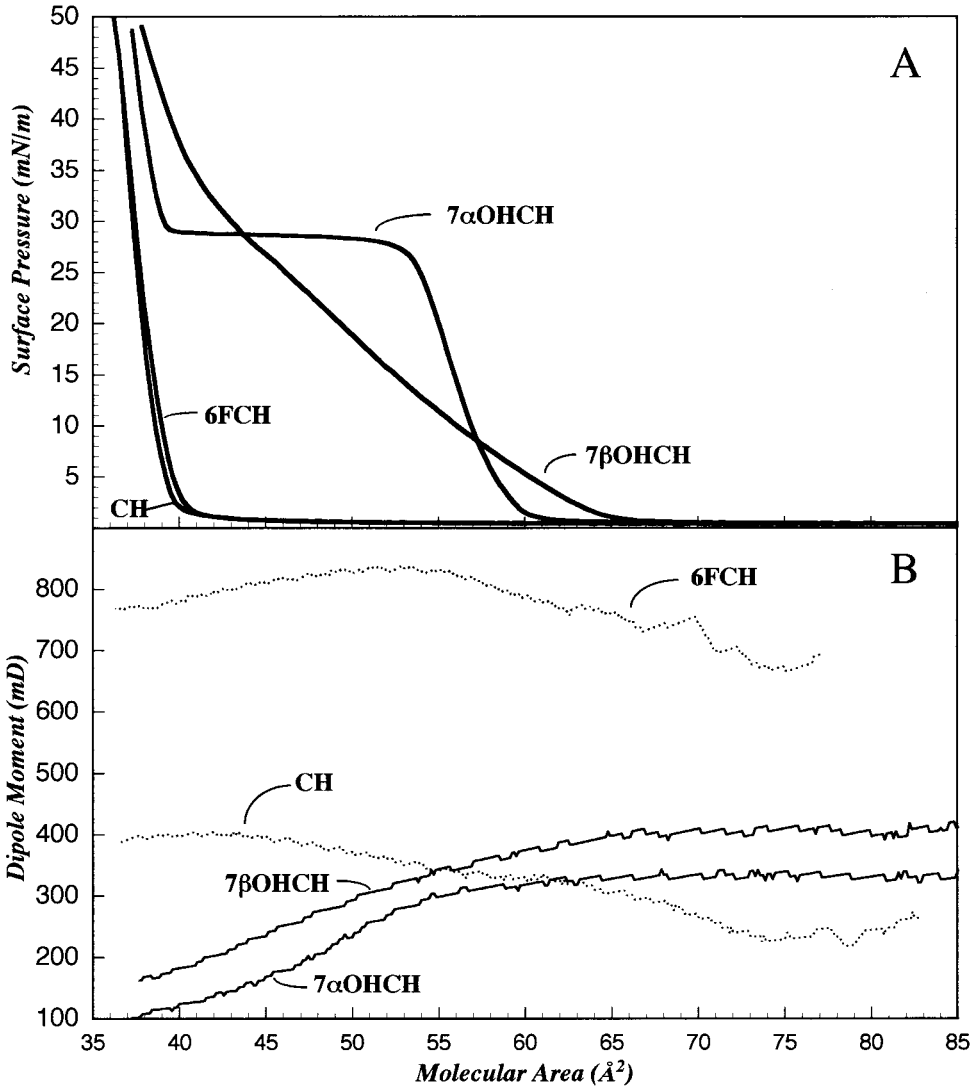

Fig. 1. Surface pressure (π)−area (A) isotherms (A) and surface potentials (B) and for 7αOHCH, 7βOHCH, 6FCH, and CH. Subphase conditions were 5 m NaCl at pH 3, T = 21 ± 0.5°C. Isotherms of CH and 6FCH are virtually superimposable, whereas 7αOHCH and 7βOHCH demonstrate lift-off areas of 59 and 64 Å^2, respectively. The isotherm of 7αOHCH exhibits a liquid expanded–liquid condensed phase transition near a pressure of 28 mN/m before rising sharply again to approach the isotherm of CH as a solid condensed film. The curve of 7βOHCH gradually increases to approach the isotherm of CH near 50 mN/m. Surface potentials (B) of 7αOHCH and 7βOHCH are initially flat, but slope negatively near 55 Å^2 for 7αOHCH, and near 65 Å^2 for 7βOHCH. As these changes in surface potentials occur, the $\pi-A$ isotherms display lift-offs in surface pressure.

typical of liquid expanded films. In the case of 7αOHCH, lift-off occurs at 59 Å^2 and π rises rapidly before reaching a liquid expanded–liquid condensed phase transition between molecular areas of 54 and 39 Å^2. Below molecular areas of 39 Å^2, the surface pressure rises sharply as the monolayer is compressed in the two-dimensional solid state. The mean molecular area of 7αOHCH in the solid state at pressures near 50 mN/m remains 1.7 Å^2 larger than CH, consistent with the additive size of a hydrated OH group projecting from the side of the sterol ring system. Lift-off of the isotherm for 7βOHCH occurs at 64 Å^2 and displays a continuous upward sweep until the CH isotherm is approached at a surface pressure of ≈50 mN/m.

Figure 1B demonstrates that the mD value of 6FCH is nearly twice that of CH, and both dipole moments have a slightly positive slope as the surface area is reduced. This is consistent with the additive dipole vectors of F and 3-OH on the sterol nucleus. The slope of the surface potential of 7βOHCH is initially flat at high molecular areas (B), but declines below 65 Å^2/molecule, which corresponds to the lift-off in the isotherm (panel A). In contrast, the surface dipole moment of 7αOHCH (B) is initially flat to ≈55 Å^2/molecule, and then declines sharply, consistent with compression to the liquid condensed state between 54 and 39 Å^2. The nucleus-substituted 6FCH and 7OHCHs demonstrated no evidence of crystallization or gelation even at

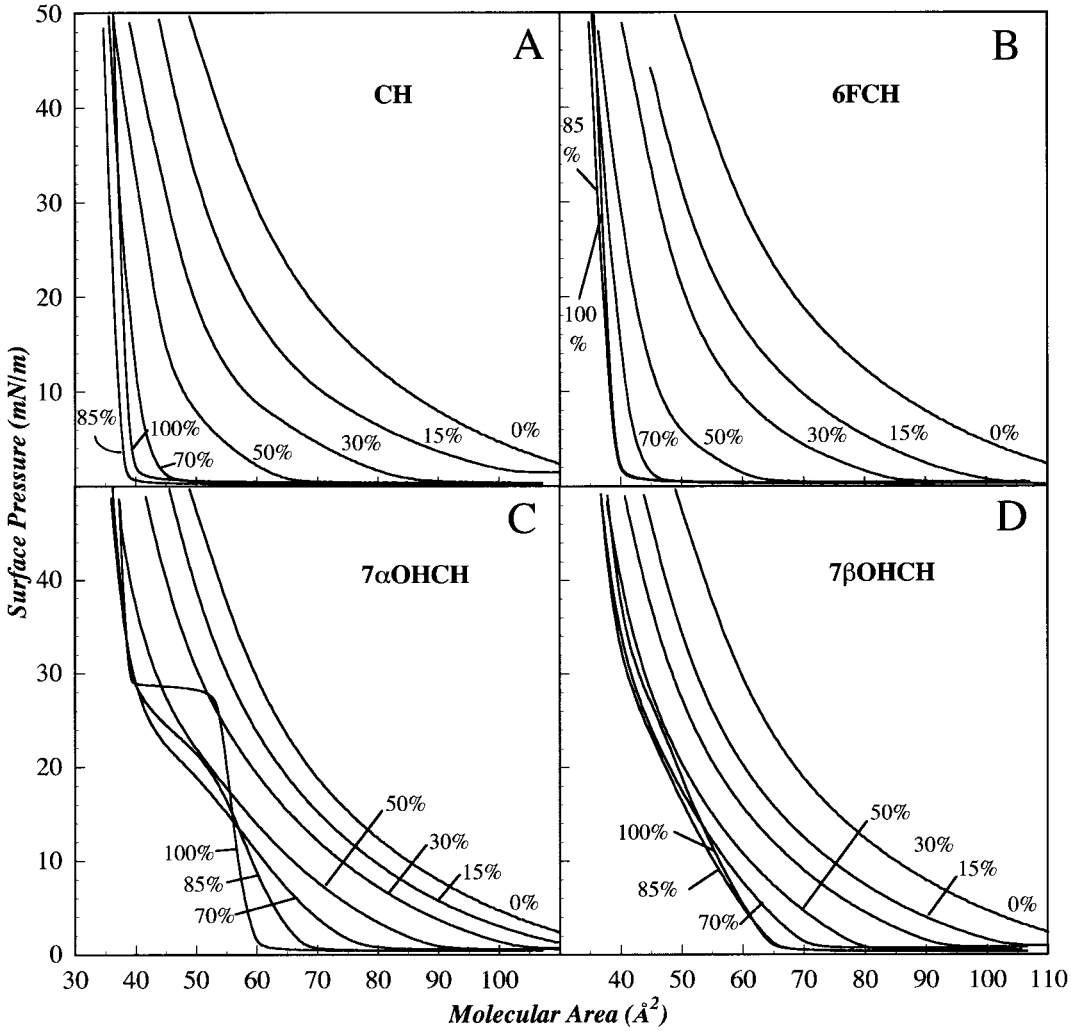

Fig. 2. Surface $\pi-A$ isotherms of monolayers of binary mixtures of CH (A), 6FCH (B), 7αOHCH (C), 7βOHCH (D), and POPC with mole percent sterol indicated on each curve. The shape of the CH and 6FCH curves are similar, except the 85% CH isotherm is shifted to a smaller molecular area than 100% CH. Isotherms of 7αOHCH (C) in mixtures with POPC demonstrate attenuated phase transitions in the 85% and 70% sterol mixtures, suggesting that the orientation of the OHCH remains tilted at the interface.

the highest compressions, ≈50 mN/m, indicating that the molecules remain as monolayers.

Figure 2 (A–D) depicts the $\pi-A$ isotherms of binary mixtures of CH, 6FCH, 7αOHCH, and 7βOHCH with POPC. The isotherms for CH (A) and 6FCH (B) are virtually identical except that at 85% CH (A), the isotherm is shifted to the left of the 100% CH curve, whereas below a pressure of 20 mN/m, the 85% 6FCH isotherm (B) overlies the 100% 6FCH curve. At each percent sterol examined, $\pi-A$ isotherms of 7αOHCH (C) and 7βOHCH (D) with POPC are shifted to larger molecular areas than isotherms of CH or 6FCH with POPC (A and B, respectively). The marked phase transition from a liquid expanded to a liquid condensed state between 54 Å^2 and 39 Å^2 in the 100% 7αOHCH isotherm (C) is less obvious in the 85% and 70% sterol–POPC mixtures, and eliminated at 50% 7αOHCH. Although in all mixtures of 7αOHCH (C) and 7βOHCH (D) with POPC, the curves are shifted incrementally to higher molecular areas than mixtures of CH (A) or 6FCH (B) with POPC, this is particularly true at pressures less than 30 mN/m.

Figure 3 plots additivity curves for binary mixtures of CH, 6FCH, 7αOHCH, and 7βOHCH with POPC at a constant pressure of 10 mN/m. The dashed lines represent ideal additivity. In all mixtures of CH or 6FCH with POPC, the curves deviate negatively from ideality to virtually identical degrees. This indicates that the mixed monolayers of 6FCH or CH with POPC result in a hemimembrane with a smaller mean molecular area than that produced by either lipid alone, suggesting ordering of the acyl chains of POPC, making them less fluid and more dense. With respect to the OH-substituted CHs, 7βOHCH induces appreciably greater negative deviation than 7αOHCH, but at all mol % the extent is less than in mixtures of CH or 6FCH with POPC. At equimolar mixtures of sterol and POPC, CH and 6FCH condense by 14 and 15 Å^2, respectively, compared to 5 and 10 Å^2, in the case of 7αOHCH and 7βOHCH, respectively. Although both 7αOHCH and

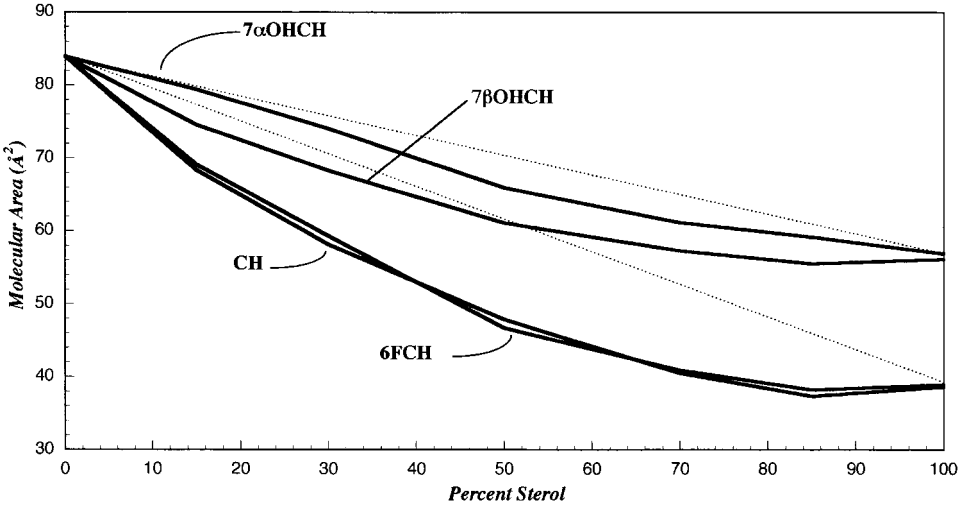

Fig. 3. Area-additivity curves for POPC in binary mixtures with CH, 6FCH, 7αOHCH, and 7βOHCH. Mole fractions are plotted against molecular area, with the surface pressure constant at 10 mN/m. Dashed lines represent ideal additivity of the molecular areas of POPC with the sterols. Curves for 6FCH and CH are essentially identical. Although only slight negative deviations from ideality occur with 7αOHCH, particularly with less than 30 mol% sterol, 7βOHCH demonstrates moderate negative deviations from ideality in all mixtures.

7βOHCH induce greatest condensation around 50 mol %, condensation by 7αOHCH is minimal at sterol mol fractions of 15 and 30%. When the curves of binary mixtures of CH, 6FCH, 7αOHCH, and 7βOHCH with POPC at 30 mN/m were plotted (data not shown), the negative deviations and rank ordering remained the same. Notably, at this higher π value, both 7OHCH molecules are oriented vertically (see Fig. 1).

Side chain-substituted cholesterols

Figure 4A displays the $\pi-A$ isotherms of monolayers of 25OHCH, 27OHCH, 25FCH, HeptaFCH, and CH. Three features of these isotherms distinguish the chain-substituted OHCHs from CH and its side-chain FCH analogues. First, at high molecular areas, 25OHCH and 27OHCH demonstrate elevated baseline pressures of between 1.5 and 3 mN/m, compared to less than 0.3 for CH and 6FCH. Second, the lift-offs for 25OHCH and 27OHCH occur at 36.5 and 38 Å^2/molecule, respectively, areas appreciably less than those observed with CH (39.5 Å^2). Third, in contrast to CH which does not collapse, isotherms of both 25OHCH and 27OHCH collapse between 34 and 35 Å^2/molecule. Although the areas at collapse of 25OHCH and 27OHCH are similar (Fig. 4), the collapse pressures are different, 33 mN/m and 25 mN/m, respectively. This suggests, therefore, that 25OHCH and 27OHCH molecules bond with different affinities to the interface, with 25OHCH > 27OHCH. Further compression of 25OHCH below 35 Å^2/molecule produces a gradual rise in pressure, whereas compression of 27OHCH produces a plateau. Qualitative viscosity experiments carried out by observing the movement of talc sprinkled on the interface (see Experimental Procedures), are consistent with crystallization of both lipids, indicating multimolecular layer formation. In contrast to the OHCHs, $\pi-A$ isotherms of 25FCH, HeptaFCH, and CH are essentially identical to each other (Fig. 4A), showing similar baseline π and no collapse, but slight expansion of HeptaFCH between surface pressures of 1 and 15 mN/m.

Figure 4B demonstrates that the dipole moments for 25OHCH and 27OHCH are essentially flat until molecular areas below 38 Å^2 are reached, beyond which they decline appreciably. This breakpoint corresponds to molecular areas at which lift-off occurs (Fig. 4A). At collapse of the monolayers, dipole moments begin their steepest decline. Although surface dipole moments of 25FCH and CH are similar in shape to each other, 25FCH has a lower dipole moment than CH, possibly reflecting the dipole vector of the side chain F that partially cancels that of the 3OH group. Perhaps for similar reasons, this effect is greatly amplified in HeptaFCH, where the dipole moment is a large negative value throughout compression and curves downwards from high molecular areas.

Figure 5 (main plot) displays expanded $\pi-A$ isotherms of 25OHCH and 27OHCH to show that the elevated baseline pressures persist even at 250 Å^2/molecule. Further, they reveal gradual increases in surface pressure during compression from 200 to 100 Å^2/molecule. Inset (A) shows that between 200 and 140 Å^2/molecule, dipole moments rise nearly 50 mD. Inset (B) depicts isotherms expanded on the *y*-axis to reveal increases in π that parallel elevations in dipole moments in (A). Taken together, the isotherms and dipole moments suggest that at low surface concentrations, i.e., large molecular areas, 25OHCH and 27OHCH are oriented parallel to the interface with the side-chain OH and 3-OH groups H-bonded to the interface. With compression of the monolayer in the 140 to 200 Å^2 range, both OHCHs assume a vertical orientation through lateral collisions with adjacent molecules, most

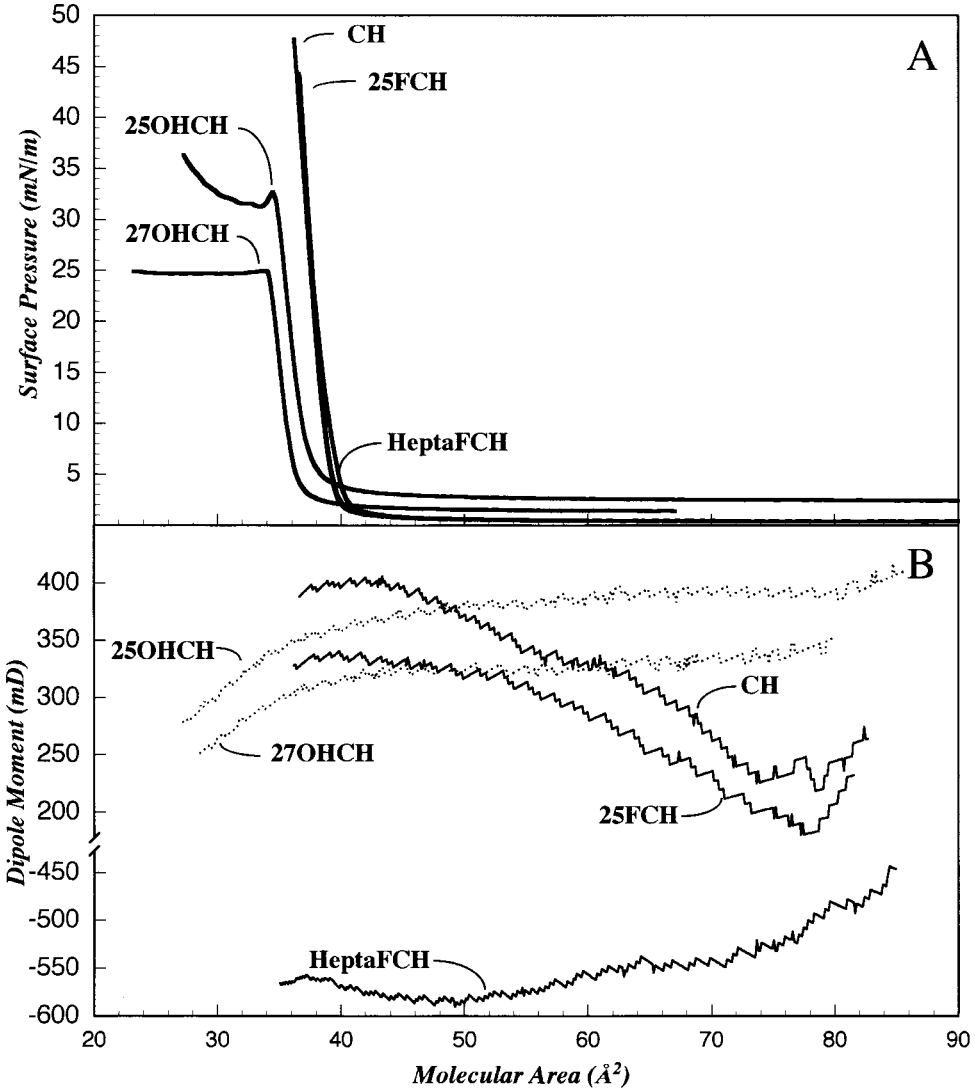

Fig. 4. The upper panel (A) displays $\pi-A$ isotherms of CH and 25FCH that are virtually superimposable, compared to HeptaFCH which is slightly expanded at low surface pressures. Both 25OHCH and 27OHCH exhibit elevated baseline pressures and lift-offs at smaller molecular areas than CH. The isotherms of 25OHCH and 27OHCH show abrupt phase transitions at $\leq$35 Å^2, coinciding with evidence of crystallization at the interface. The lower panel (B) depicts surface potentials of pure CH, 25FCH, 25OHCH, 27OHCH, and HeptaFCH. For the sake of clarity, potentials of the OHCHs are represented by dotted lines. In a fashion similar to CH and 6FCH in Fig. 1, the potential of 25FCH rises initially, then levels off as the monolayer condenses into a solid film. The dipole moment for HeptaFCH is highly negative, resulting from the polarization of the fluorinated side chain. At condensation of 25FCH into a solid film, its dipole moment is 50 mD smaller than that of CH, whereas the dipole of HeptaFCH is approximately 800 mD lower than that of CH. Surface potentials of both OHCHs decline precipitously at molecular areas less than 38 Å^2, coincident with phase transitions in the isotherms (A).

likely with the side-chain OH group in each case acting as the interfacial anchor (evidence discussed below).

Figure 6 (A–D) depicts $\pi-A$ isotherms of binary mixtures of 25FCH, HeptaFCH, 25OHCH, and 27OHCH with POPC. The isotherms of 25FCH and HeptaFCH with POPC are similar to each other, although for 85% 25FCH, like 85% CH (Fig. 2A), the isotherm is shifted to a smaller molecular area compared to the 100% curve. Isotherms of 25OHCH or 27OHCH in all molar ratios with POPC reveal persistence of the elevated baseline pressures present in the 100% OHCH curves. Figures 6C and 6D demonstrate that the collapse pressures of 25OHCH and 27OHCH occur at higher π values with decreasing % sterol and are eliminated in the 30% sterol mixtures, whereas the molecular areas at collapse remain constant. These increasing collapse pressures with increasing POPC represent classical "envelope curves" (28), and suggest intimate miscibility of OHCHs with POPC.

Figure 7 depicts additivity curves of 25OHCH, 27OHCH, 25FCH, HeptaFCH, and CH with POPC at 10 mN/m. Curves for both 25FCH and CH are similar to each other, displaying considerable negative deviations from ideality at all mol % sterol, indicating strong condensation of the POPC monolayers. Over all molar ratios, the HeptaFCH curve deviates negatively from ideal-

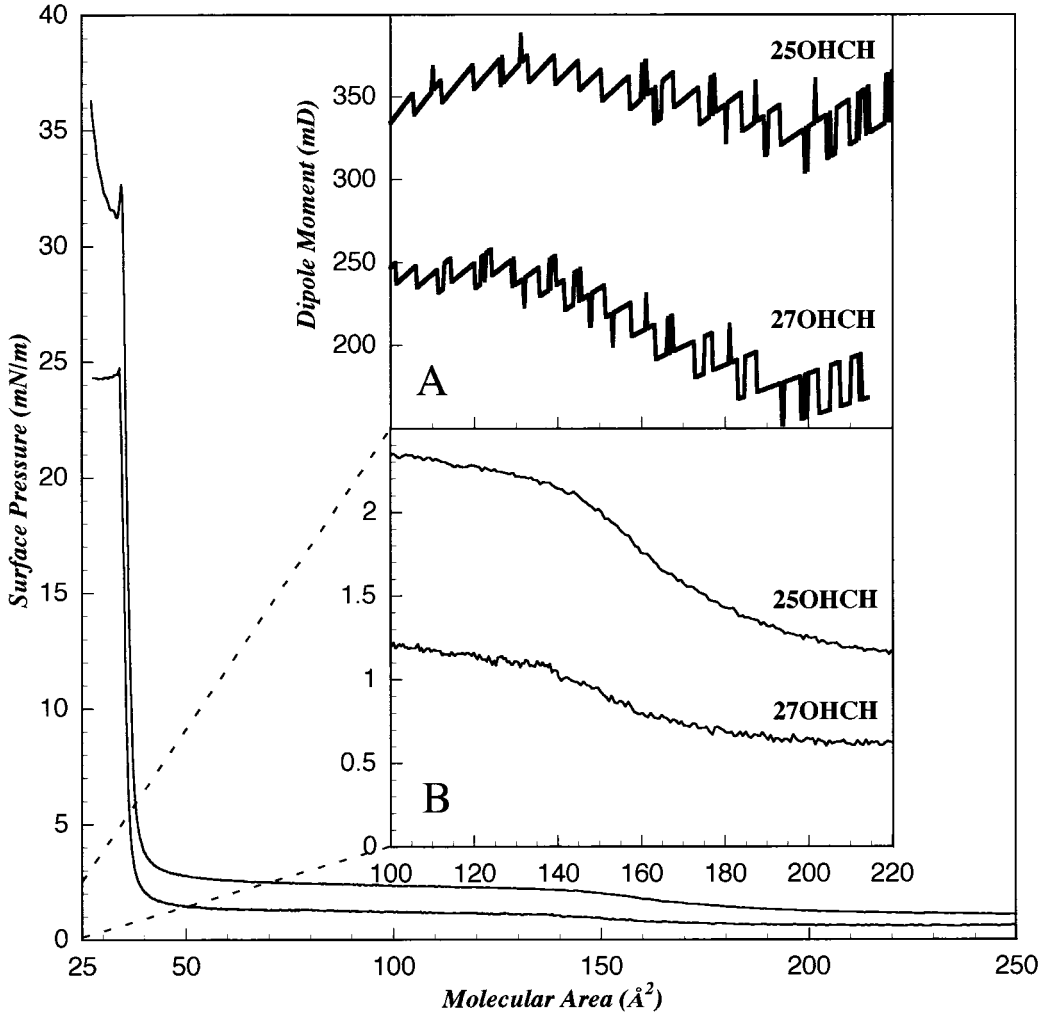

Fig. 5. Expanded $\pi - A$ isotherms of 25OHCH and 27OHCH ranging from molecular areas of 250 to 25 Å^2. Graphs in inset (A) depict surface dipole moments and (B) isotherms between molecular areas of 100 and 220 Å^2. Inset (A) demonstrates the increases of nearly 50 mD in dipole moments for each hydroxysterol between molecular areas of 200 and 140 Å^2. Inset (B) (*y*-axis expanded between surface pressures of 0 and 2.5) reveals appreciable increases in surface pressure that parallel the elevations in dipole moments (A). At molecular areas greater than 190 Å^2, the OHCHs molecules are most likely oriented horizontally at the interface. With compression of the monolayer, the sterol nuclei of molecules lift out of the interface, changing from horizontal to vertical orientations (see Discussion).

ity, although to a lesser degree than observed with CH or 25FCH. This suggests that either the slightly increased radii of the seven F atoms on the side chain or their aggregate polarity prevent tight packing of the mixed monolayer as observed with 25FCH or CH and POPC. In contrast, at 15 mol% sterol, both 25OHCH and 27OHCH show expansion of the mixed sterol/POPC monolayer, and condensation at mixtures containing >30 mol% OHCH. At molar ratios of 70–85 mol%, 25OHCH and 27OHCH display substantial negative deviations from ideality similar in magnitude to CH or 25FCH with POPC. This indicates distinctly different molecular interactions at low, compared to high, ratios of side-chain OHCH to POPC, and is most likely explained by acyl chain-OH repulsion at low sterol concentrations, with direct OHCH–OHCH interactions shielding the electronegative OH groups at higher sterol concentrations.

DISCUSSION

The surface chemistry of fluorinated analogues of biological lipids has shown that highly fluorinated phosphatidylcholines exhibit interfacial stability, with higher collapse pressures than their hydrocarbon analogues (29). In fact, perfluoro-*n*-eicosane, in the absence of a classic polar function, displays ordering at an interface (30). In the present study, we sought to characterize the orientation, size, and molecular interactions in monolayers of one poly- and two mono-FCHs, alone and with POPC, a common membrane lecithin. To compare electronegative substitutions other then F at similar locations on the sterol nucleus and side chain, four physiologically relevant OHCHs were studied and compared to the F analogues. Both 7αOHCH and 25OHCH are important intermediates in the bile acid synthetic pathways (31), whereas 27OHCH, synthesized by sterol 27-hydroxylase,

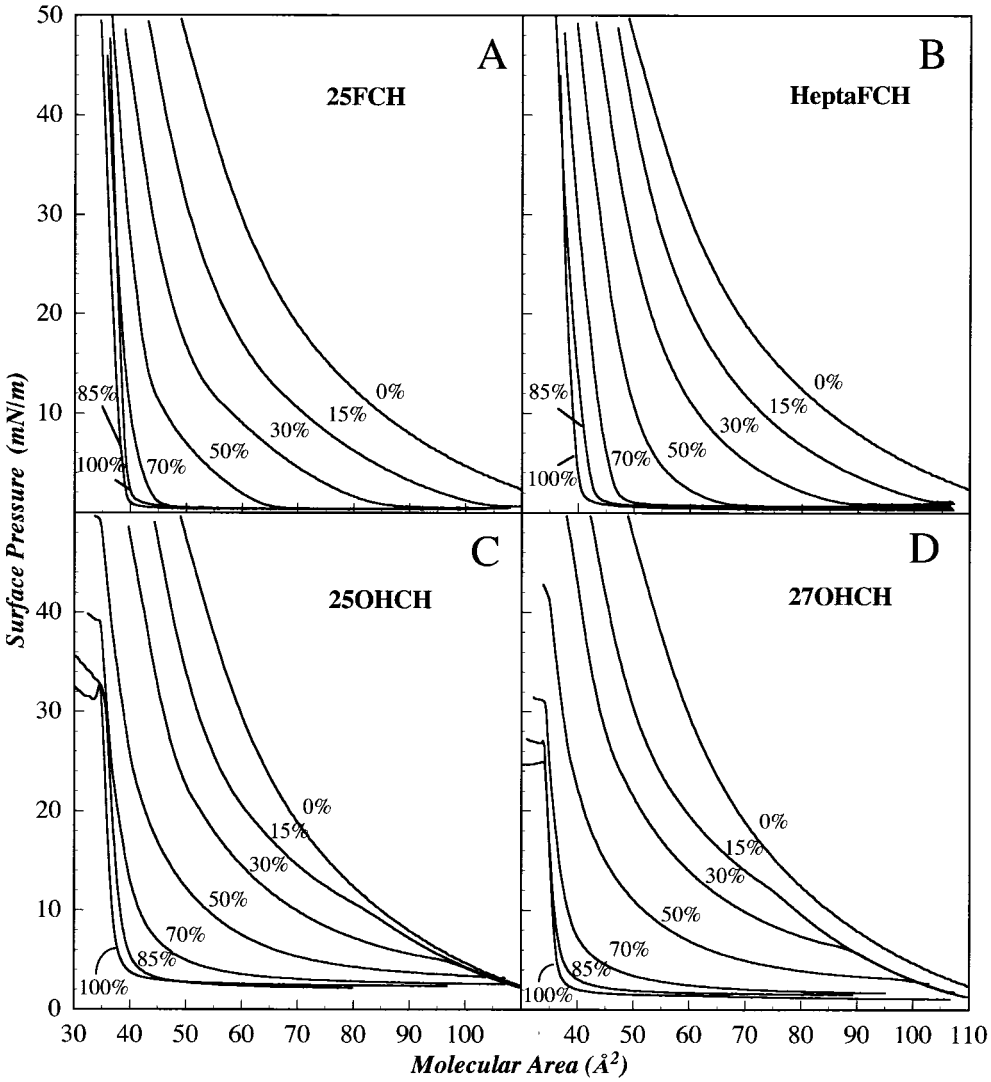

Fig. 6. Surface $\pi-A$ isotherms of binary mixtures of 25FCH, HeptaFCH, 25OHCH, 27OHCH, and POPC with mole percent sterol indicated on each curve. Isotherms of 25FCH and HeptaFCH are similar to CH and 6FCH in Fig. 2. As noted with CH, the 85% 25FCH mixture is shifted to a smaller molecular area compared with the 100% 25FCH curve. The phase transitions observed with 25OHCH and 27OHCH occur at higher pressures with increasing POPC concentrations, and are eliminated in mixtures > 50% POPC.

is found in most tissues including plasma and atheromatous plaques (32).

Monolayers of pure cholesterol and its substituted analogues

Binary systems composed of CH and several lecithins have been characterized by using the Langmuir-Pockels surface balance and surface potential measurements (12, 13, 19, 33–38). Our $\pi-A$ isotherms and surface dipole data demonstrate that the molecular areas of CH, 6FCH, 25FCH, and HeptaFCH are comparable. Like CH, the FCHs are vertically oriented at the interface throughout compression from the liquid to the solid state, with the 3-OH group providing a hydrophilic anchor to the polar interface. The similar molecular areas of FCH and CH can be accounted for by the small steric change induced by a F substituent, and this suggests that despite its hydrophilic nature, it is not repelled by hydrophobic interactions with neighboring molecules. The lift-offs of 7αOHCH and 7βOHCH at molecular areas greater than 60 Å^2 (Fig. 1) are consistent with tilting of the molecules at the interface, with both 7 α/β- and 3-OH groups in the interface. Although the shape of these isotherms is in agreement with limited previous work on both 7-OHCHs (13), differences in the plateau pressure of 7αOHCH are likely due to differing experimental conditions, including subphase compositions and pH. We depict through molecular modeling in **Fig. 8** the interfacial orientation of 7αOHCH and 7βOHCH molecules. This shows that the 7α-OH projection results in closer approximation of the 7-OH group to the interface than is permitted with the 7β-OH projection, which brings the hydrophobic carbons of the A/B rings adjacent to the interface. This results in stronger interfacial H-bonding to the 7α-OH than the 7β-OH on the

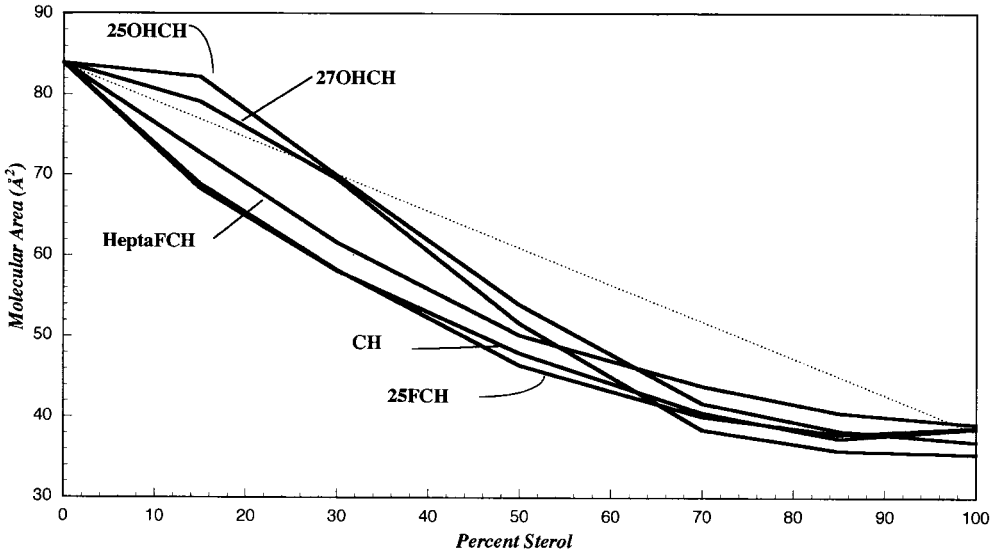

Fig. 7. Additivity curves for binary mixtures of CH, 25FCH, 25OHCH, 27OHCH, and HeptaFCH with POPC. Molecular areas are plotted against mole percent sterol at a constant surface pressure (10 mN/m). The dotted line represents ideal additivity for the molecular areas of sterol mixtures with POPC. Additivity curves of both OHCHs are biphasic, displaying expansion of the monolayer at 15 mol% and condensation at percentages >30 mol%. Both CH and 25FCH molecules condense POPC to a similar degree at all concentrations, whereas HeptaFCH induces less condensation.

sterol nucleus. The surface potential of 7α-OHCH (Fig. 1B) does not fall appreciably until surface pressures between 27–29 mN/m (Fig. 1A) are reached, suggesting that the 7α-OH group is strongly anchored in the interface. In contrast, the area at lift-off (Fig. 1A) and decline in the surface potential (Fig. 1B) of the 7β-OH isomer suggest that the 7OH function is dislodged from the interface at 64 Å^2, further supporting the stronger bonding of

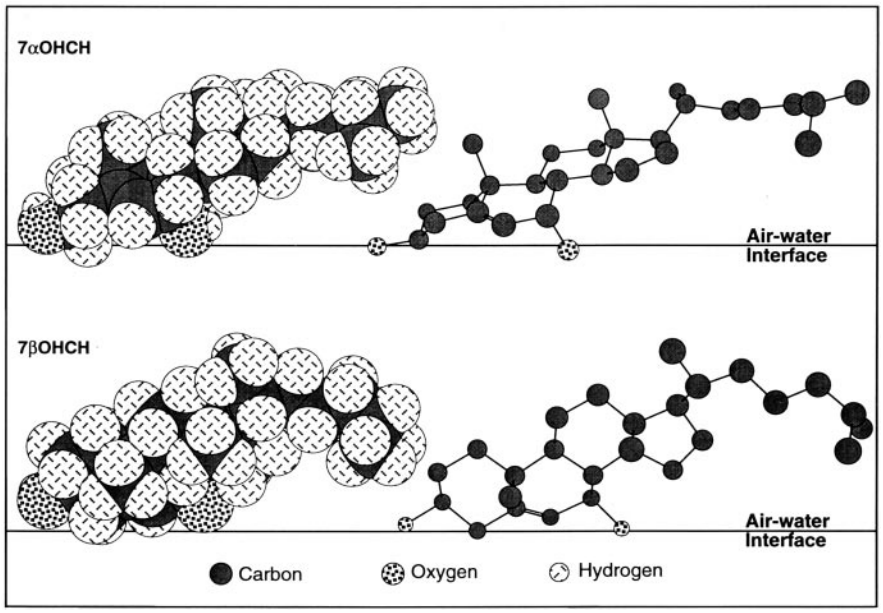

Fig. 8. Three-dimensional space-filling molecular models (on the left) of 7αOHCH and 7βOHCH at the air–water interface showing all atoms. Molecular models (on right) are ball and stick without displaying hydrogen atoms. Energy minimization indicates that the 7α-OH projection permits closer approximation of the sterol rings to the interface, thereby allowing maximization of hydrogen bonding between the OH-group and the interface. In contrast, the 7β-OH projection brings the A/B rings, and especially the hydrophobic C4 and C6 atoms into the interface, thereby limiting hydrogen bonding of the 7OH-group with the interface. In mixtures with POPC, these 7OHCHs, which are tilted toward the interface because of the H-bonding of the 7OH group, do not condense the mixed monolayers as effectively as CH.

the 7α-OH group to the interface compared with the 7β-OH group. Once the 7-OH groups are lifted out of the interface completely, both sterols become oriented vertically at the interface (Fig. 1A).

The behavior of the isotherms or the side chain OHCHs (Fig. 5) suggests that like the dihydroxy bile acids (21), 25OHCH and 27OHCH are oriented horizontally at the interface at large molecular areas (>140 Å^2), with the 3-OH and the side chain OH anchored to the interface. Also based on surface balance experiments, the horizontal orientation of 22,*R*-OHCH, another side chain OHCH, has been suggested, because of a lift-off at 103 Å^2/molecule (39). This contrasts with 22,*S*-OHCH or 20,*S*-OHCH, which appear to orient vertically at large molecular areas (39). In our work, the slight rises in surface pressures between 140 and 200 Å^2/molecule from 0.7 and 1.2 mN/m to 1.1 and 2.2 mN/m for 27OHCH and 25OHCH, respectively, compared to the sharp rise with 22,*R*-OHCH (39), are consistent with the entire side chain of these terminally hydroxylated sterols lying horizontal at the interface. In this configuration, the side chain will undergo *cis-trans* conformational isomerizations and alter its length. In the case of 22,*R*-OHCH, the C23–27 chain most likely orients vertically, resulting in no contribution to interfacial molecular area from side chain isomerizations. With progressive compression of 25OHCH and 27OHCH monolayers, the weakest H-bonds at the interface break first, forcing the sterol to become vertically oriented and apparently resulting in the 3-OH group projecting into the hydrophobic environment (air). The smaller molecular area at lift-off and the elevated baseline pressure of 25OHCH are consistent findings that we also found with 27OHCH, and which were not noted in previous work (13).

Evidence for the interfacial anchoring of 25OHCH and 27OHCH by the side chain OH group is suggested strongly by the data in Figs. 4 and 5. First, the transition from horizontal to vertical orientation for both sterols occurs in the same range of molecular areas (Fig. 5B), suggesting that the energy necessary to force an OH group out of the interface is the same. Second, both OHCHs lift off at smaller molecular areas than CH (Fig. 4A); because the sterol ring is the principal contributor to the molecular area, this suggests that the molecules are not vertically oriented in the same manner as CH or the FCHs, namely that the 3-OH group does not provide the interfacial anchor. Third, collapse points, not observed with CH (Fig. 4A), occur at different surface pressures with 25OHCH and 27OHCH, pointing toward distinctly different energies necessary to pull the anchoring OH out of the interface. Taken together, these surface balance data suggest that the side chain OH groups provide the interfacial anchors when these OHCHs become vertical during monolayer compression. As noted elsewhere (14, 21, 40), cholanoic acid, a bile acid with a C24 COOH group and no OH group on the sterol nucleus, is oriented with the side chain anchored in the interface, and its $\pi-A$ isotherm closely resembles those of 25OHCH and 27OHCH. We suggest schematically in **Fig. 9** that the interfacial "reverse orientation" of 25OHCH and 27OHCH would permit smaller molecular areas than CH (Fig. 4A), because the side chain *cis-trans* conformational isomerizations would allow variable distances between the sterol nucleus and the interface, creating a staggered layer of molecules with more condensed packing. The slightly lower surface pressure where 27OHCH collapses suggests that the 25OH group is H-bonded more tightly to the interface than the 27OH group.

Monolayers of sterol/POPC mixtures

As assessed by microviscosity measurements using the fluorescent probe 1,6-diphenyl-1,3,5-hexatriene, membrane fluidity of multilamellar vesicles composed of egg lecithin and 6FCH was not significantly altered compared to CH (9). This is consistent with the present work where all FCHs exhibited interfacial properties similar to CH, with 6FCH and 25FCH condensing monolayers of POPC in a manner virtually indistinguishable from CH, and with HeptaFCH having a somewhat lesser effect (Fig. 7). Because the CH side chain is so much smaller than the rigid sterol ring system, and the radius of F is only 0.2 Å larger than H, it was not expected that F substitution on the side chain would augment the interfacial area of pure HeptaFCH in monolayers (Fig. 4A). However, the reduced condensation of POPC in binary mixtures with HeptaFCH compared to CH most likely reflects the increased hydrophilic nature of the 7 F atoms on the HeptaFCH side chain, as suggested by its accelerated mobility on reversed phase HPLC (7, 27).

Although both 7αOHCH and 7βOHCH induce condensation of POPC at 10 mN/m, the effect is less than with CH or the FCHs, and minimal at concentrations <30 mol% 7αOHCH (Fig. 3). The "tilted" sterol orientation at the interface appears to persist in mixtures with POPC, particularly at high OHCH concentrations. This is evidenced by the blunted phase transition from a liquid expanded to a liquid condensed state in the 85% and 70% sterol mixtures (Fig. 2C and D). The decreased capacity to condense the mixed monolayer most likely represents the inability of the "tilted" sterols to intercalate effectively within the hemimembrane. The "reverse orientation" of 25OHCH and 27OHCH appears to be maintained in binary mixtures with POPC, because the surface pressures at collapse of both OHCHs rise with increasing mol % POPC (Fig. 6C and D), suggesting intimate miscibility of POPC with 25OHCH and 27OHCH. Insight into a possible mechanism for this novel finding that the side chain OHCHs induce expansion of POPC monolayers at concentrations <30 mol% OHCH, but condensation at >30 mol% (Fig. 7) can be inferred from CH:phosphatidylcholine bulk systems. Using X-ray diffraction (41) and cholesterol oxidase probe studies (35) at CH:PC molar ratios greater than 1:1 suggest lateral phase separation with two-dimensional CH–CH clusters. By inference, at <30 mol% sterol concentrations (Fig. 7), the expansion of the monolayer is most likely due to the 3-OH groups being fully exposed to the hydrophobic acyl chains of POPC. At molar concentrations of 50% and higher, the OHCH molecules most likely phase separate into H-bonded clusters, thereby

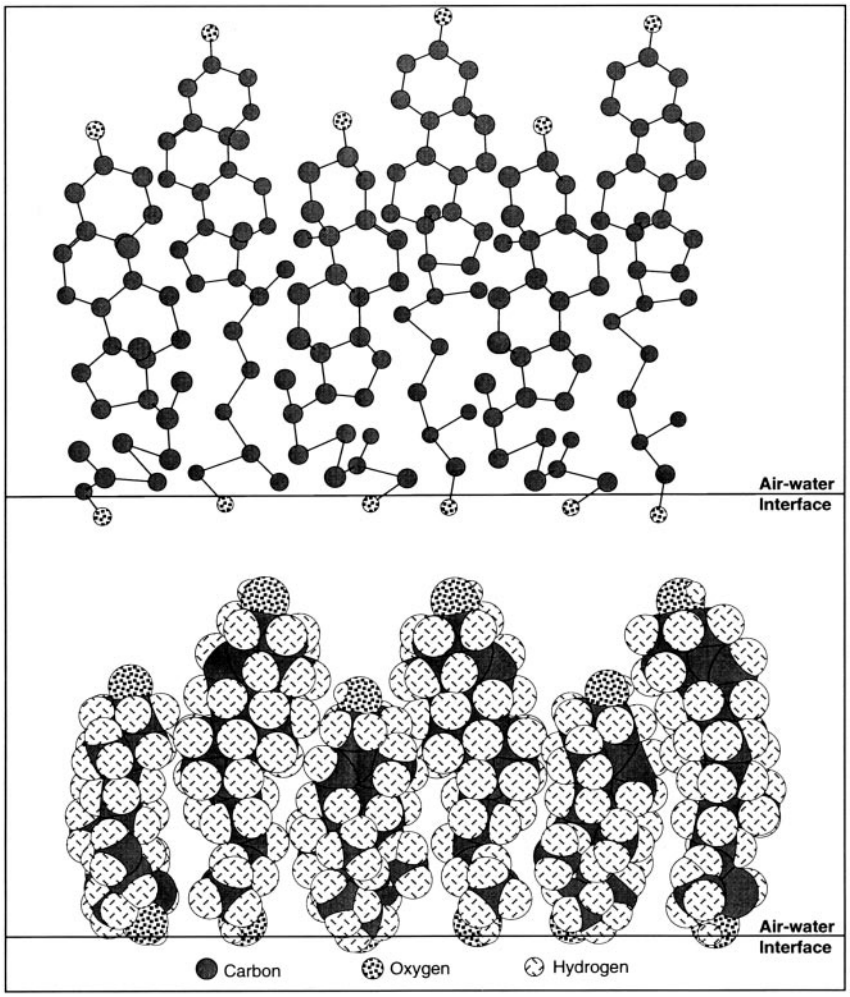

Fig. 9. Three-dimensional molecular models of 27OHCH at the air–water interface. The upper panel contains ball and stick models without displaying hydrogen atoms. The lower panel depicts space-filling molecular models showing all atoms. Molecules are oriented with the side-chain OH-group H-bonded at the interface (see Discussion for details). The bulkiest component of the molecule, the rigid sterol nucleus, can change very little in volume, whereas the side chain undergoes *cis–trans* conformational isomerizations, thereby changing the vertical dimension of the entire molecule. As inferred from the current work, with compression of the monolayer, reverse orientation of the molecules occurs; that is the 3-OH group projects away from the interface, whereas the side chain-OH is anchored in the interface. Because of this configuration, the sterol side chain length is highly variable and results in tighter packing of the monolayer films, producing a smaller molecular area of 27OHCH (and 25OHCH) compared with CH or FCHs films (see Discussion and Fig. 4).

shielding the 3-OH groups from the acyl chains of POPC. Although this behavior was not detected previously by another group (13) with 25OHCH and dioleoylphosphatidylcholine (DOPC), only 3 molar mixtures of 25OHCH with DOPC were examined, so the phenomenon may have been missed. Nonetheless, between 2.5 and 30% 25OHCH, glucose permeability in the 25OHCH–lecithin liposomes was greater than for egg lecithin alone (13), which corresponds to the region where we found that 25OHCH and 27OHCH induced expansion of the POPC monolayer.

In summary, these data suggest that fluorine substitution of CH at either the nucleus or side chain sites, or indeed even heptafluorination of the side chain, preserves the interfacial properties of CH, including molecular size, orientation, intercalation into and condensation of POPC membranes. In marked contrast to the side chain OHCHs, all FCHs form solid condensed films, like CH, with no collapse upon compression. Because of their second hydrophilic OH group, the OHCHs demonstrate markedly different properties depending on whether the OH group is on the side chain or sterol nucleus. Of potential biomolecular relevance is the reverse orientation of the 25OHCH and 27OHCH anchored to the interface by the side chain OH, which may expose the side chain, usually deep within a membrane bilayer in the case of CH, to enzymes and receptors at membrane surfaces. Compared with CH, the interfacial tilting of both 7OHCHs results in larger molecular areas and decreased condensation effects on POPC monolayers. This may result in vivo in increased membrane permeability and extrusion of CH from membranes

such as the endoplasmic reticulum after 7α-hydroxylation, the rate-limiting step during bile acid synthesis.

The value of fluorinated analogues as tracer compounds is intrinsically linked to and depends on their physical–chemical and biochemical similarity to their hydrocarbon analogues. If these molecules retain the three-dimensional molecular structure and chemical reactivity of the native compound, they may prove to be ideal probes for tracking uptake, metabolism, and disposition at the ultrastructural level (23, 24). The FCHs, with properties highly similar to CH, may serve as tracer compounds for CH, while preserving essential membrane properties. By site-specific F substitution, with placement of the highly stable C–F bond at or near a reactive site, functional groups and the enzymatic pathways and receptor sites used by them can be targeted. Moreover, as several steroids, including OHCHs and bile acids (42–44) are established ligands for orphan nuclear receptors, it may be advantageous to block specific catabolic mechanisms of these compounds by F substitution. Therefore, because of the CH-mimetic hemimembrane properties, FCHs may provide a novel class of molecules that permits visualization and the potential for tracking CH, while selectively blocking enzymatic pathways, including esterification and conversion into bile acids.

Supported in part by the Stanley Sarnoff Endowment, the Glaxo Wellcome Institute of Digestive Health, and NIH grants DK36588, DK34854, and DK52911. We thank Dr. William Wilson (Rice University, Houston, TX) for generously supplying the heptafluorocholesterol and Ms. Monika R. Leonard for helpful discussions.

Manuscript received 3 February 2000 and in revised form 9 March 2000.

REFERENCES

1. Bergstrom, D. E. and D. J. Swartling. 1988. Fluorine substituted analogs of nucleic acid components. *In* Fluorine-Containing Molecules: Structure, Reactivity, Synthesis, and Applications. J. F. Liebman and A. Greenberg, editors. VCH Publishers, Inc. New York, NY. 259–308.
2. Bondi, A. 1964. van der Waals volumes and radii. *J. Phys Chem.* **68:** 441–451.
3. Goldman, P. 1969. The carbon-fluorine bond in compounds of biological interest. *Science.* **164:** 1123–1130.
4. Filler, R. 1986. Biologically active fluorochemicals. *J. Fluor. Chem.* **33:** 361–375.
5. Filler, R., and Y. Kobayashi. 1982. Biomedicinal Aspects of Fluorine Chemistry. Kodansha Scientific Books, Tokyo.
6. Morisaki, M., C. Duque, N. Ikekawa, and M. Shikita. 1980. Substrate specificity of adrenocortical cytochrome P-450scc—I. Effect of structural modification of cholesterol side-chain on pregnenolone production. *J. Steroid Biochem.* **13:** 545–550.
7. Wilson, W. K., S. Swaminathan, F. D. Pinkerton, N. Gerst, and G. J. Schroepfer, Jr. 1994. Inhibitors of sterol synthesis. Effects of fluorine substitution at carbon atom 25 of cholesterol on its spectral and chromatographic properties and on 3-hydroxy-3-methylglutaryl coenzyme A reductase activity in CHO-K1 cells. *Steroids.* **59:** 310–317.
8. Prestwich, G. D., M. S. Hong, and A. K. Gayen. 1983. Side chain modified sterols as probes into insect molting hormone metabolism. II: synthesis of monofluorocholesterols. *Steroids.* **41:** 79–94.
9. Zundel, M., K. P. Nambiar, G. Boswell, and K. Bloch. 1989. 6-Fluorocholesterol as a growth factor for the yeast mutant GL7. *Biochemistry.* **28:** 5161–5164.
10. Harte, R. A., S. J. Yeaman, J. McElhinney, C. J. Suckling, B. Jackson, and K. E. Suckling. 1996. Effects of novel synthetic sterol probes on enzymes of cholesterol metabolism in cell-free and cellular systems. *Chem. Phys. Lipids.* **83:** 45–59.
11. Small, D. M. 1968. A classification of biologic lipids based upon their interaction in aqueous systems. *J. Am. Oil Chem. Soc.* **45:** 108–119.
12. Gaines, G. L. J. 1966. Insoluble Monolayers at Liquid–Gas Interfaces. Wiley Interscience. New York.
13. Theunissen, J. J., R. L. Jackson, H. J. Kempen, and R. A. Demel. 1986. Membrane properties of oxysterols. Interfacial orientation, influence on membrane permeability and redistribution between membranes. *Biochim. Biophys. Acta.* **860:** 66–74.
14. Small, D. M. 1971. The physical chemistry of cholanic acids. *In* The Bile Acids. P. P. Nair and D. Kritchevsky, editors. Plenum Press, New York. 249–356.
15. Smaby, J. M., H. L. Brockman, and R. E. Brown. 1994. Cholesterol's interfacial interactions with sphingomyelins and phosphatidylcholines: hydrocarbon chain structure determines the magnitude of condensation. *Biochemistry.* **33:** 9135–9142.
16. Johnston, D. S., and D. Chapman. 1988. The properties of brain galactocerebroside monolayers. *Biochim. Biophys. Acta.* **937:** 10–22.
17. Phillips, M. C., B. D. Ladbrooke, and D. Chapman. 1970. Molecular interactions in mixed lecithin systems. *Biochim. Biophys. Acta.* **196:** 35–44.
18. Phillips, M. C. 1972. The physical state of phospholipids and cholesterol in monolayers, bilayers and membranes. *Prog. Surface Membr. Sci.* **5:** 139–221.
19. Miñones Trillo, J., S. Garcia Fernandez, and P. Sanz Pedrero. 1968. Studies on monolayers: mixed films of cholesterol and lecithin with bile acids. *J. Colloid Interface Sci.* **26:** 518–531.
20. Carey, M. C., J. C. Montet, M. C. Phillips, M. J. Armstrong, and N. A. Mazer. 1981. Thermodynamic and molecular basis for dissimilar cholesterol-solubilizing capacities by micellar solutions of bile salts: cases of sodium chenodeoxycholate and sodium ursodeoxycholate and their glycine and taurine conjugates. *Biochemistry.* **20:** 3637–3648.
21. Fahey, D. A., M. C. Carey, and J. M. Donovan. 1995. Bile acid/phosphatidylcholine interactions in mixed monomolecular layers: differences in condensation effects but not interfacial orientation between hydrophobic and hydrophilic bile acid species. *Biochemistry.* **34:** 10886–10897.
22. Ghosh, D., R. L. Lyman, and J. Tinoco. 1971. Behavior of specific natural lecithins and cholesterol at the air–water interface. *Chem. Phys. Lipids.* **7:** 173–184.
23. Costa, J. L., D. C. Joy, D. M. Maher, K. L. Kirk, and S. W. Hui. 1978. Fluorinated molecule as a tracer: difluoroserotonin in human platelets mapped by electron energy-loss spectroscopy. *Science.* **200:** 537–539.
24. Crawford, J. M., S. Barnes, R. C. Stearns, C. L. Hastings, and J. J. Godleski. 1994. Ultrastructural localization of a fluorinated bile salt in hepatocytes. *Lab. Invest.* **71:** 42–51.
25. Leapman, R. D., and N. W. Rizzo. 1999. Towards single atom analysis of biological structures. *Ultramicroscopy.* **78:** 251–268.
26. Dauben, W. G., B. Kohler, and A. Roestle. 1985. Synthesis of 6-fluorovitamin D3. *J. Org. Chem.* **50:** 2007–2010.
27. Swaminathan, S., W. K. Wilson, F. D. Pinkerton, N. Gerst, M. Ramser, and G. J. Schroepfer, Jr. 1993. Inhibitors of sterol synthesis. Chemical synthesis and properties of 3 beta-hydroxy-25,26,26,26,27,27,27-heptafluoro-5 alpha-cholest-8(14)-en-15-one and 25,26,26,26,27,27,27-heptafluorocholesterol and their effects on 3-hydroxy-3-methylglutaryl coenzyme A reductase activity in cultured mammalian cells. *J. Lipid Res.* **34:** 1805–1823.
28. Crisp, D. J. 1949. A two-dimensional phase rule. *In* Surface Chemistry. Butterworths, London. 23–35.
29. Rolland, J. P., C. Santaella, and P. Vierling. 1996. Molecular packing of highly fluorinated phosphatidylcholines in monolayers. *Chem. Phys. Lipids.* **79:** 71–77.
30. Li, M., A. A. Acero, H. Zhengqing, and S. A. Rice. 1994. Formation of an ordered Langmuir monolayer by a non-polar chain molecule. *Nature.* **367:** 151–153.
31. Russell, D. W., and K. D. Setchell. 1992. Bile acid biosynthesis. *Biochemistry.* **31:** 4737–4749.
32. Björkhem, I., O. Andersson, U. Diczfalusy, B. Sevastik, R. J. Xiu, C. Duan, and E. Lund. 1994. Atherosclerosis and sterol 27-hydroxylase: evidence for a role of this enzyme in elimination of cholesterol from human macrophages. *Proc. Natl. Acad. Sci. USA.* **91:** 8592–8596.

33. Leathes, J. 1925. The role of fats in vital phenomena II. *Lancet.* **208:** 853–856.
34. Mattjus, P., and J. P. Slotte. 1994. Availability for enzyme-catalyzed oxidation of cholesterol in mixed monolayers containing both phosphatidylcholine and sphingomyelin. *Chem. Phys. Lipids.* **71:** 73–81.
35. Slotte, J. P. 1992. Enzyme-catalyzed oxidation of cholesterol in mixed phospholipid monolayers reveals the stoichiometry at which free cholesterol clusters disappear. *Biochemistry.* **31:** 5472–5477.
36. Slotte, J. P. 1992. Enzyme-catalyzed oxidation of cholesterol in pure monolayers at the air/water interface. *Biochim. Biophys. Acta.* **1123:** 326–333.
37. Slotte, J. P. 1995. Lateral domain formation in mixed monolayers containing cholesterol and dipalmitoylphosphatidylcholine or N-palmitoylsphingomyelin. *Biochim. Biophys. Acta.* **1235:** 419–427.
38. Stillwell, W., W. D. Ehringer, A. C. Dumaual, and S. R. Wassall. 1994. Cholesterol condensation of alpha-linolenic and gamma-linolenic acid-containing phosphatidylcholine monolayers and bilayers. *Biochim. Biophys. Acta.* **1214:** 131–136.
39. Gallay, J., B. de Kruijff, and R. A. Demel. 1984. Sterol-phospholipid interactions in model membranes. Effect of polar group substitutions in the cholesterol side-chain at C20 and C22. *Biochim. Biophys. Acta.* **769:** 96–104.
40. Ekwall, E., R. Ekholm, and A. Norman. 1957. Surface balance studies of bile acid monolayers II. Monolayers of litocholic and glycolitocholic acids. *Acta. Chem. Scand.* **11:** 703–709.
41. Lecuyer, H., and D. G. Dervichian. 1969. Structure of aqueous mixtures of lecithin and cholesterol. *J. Mol. Biol.* **45:** 39–57.
42. Lala, D. S., P. M. Syka, S. B. Lazarchik, D. J. Mangelsdorf, K. L. Parker, and R. A. Heyman. 1997. Activation of the orphan nuclear receptor steroidogenic factor 1 by oxysterols. *Proc. Natl. Acad. Sci. USA.* **94:** 4895–4900.
43. Parks, D. J., S. G. Blanchard, R. K. Bledsoe, G. Chandra, T. G. Consler, S. A. Kliewer, J. B. Stimmel, T. M. Willson, A. M. Zavacki, D. D. Moore, and J. M. Lehmann. 1999. Bile acids: natural ligands for an orphan nuclear receptor. *Science.* **284:** 1365–1368.
44. Wang, H., J. Chen, K. Hollister, L. C. Sowers, and B. M. Forman. 1999. Endogenous bile acids are ligands for the nuclear receptor FXR/BAR. *Mol. Cell.* **3:** 543–553.